Scripta Materialia 146 (2018) 150–153

Contents lists available at ScienceDirect

Scripta Materialia

journal homepage: www.elsevier.com/locate/scriptamat

Regular article

On the multiaxial yielding and hardness to yield stress relation of nanoporous gold

K.R. Mangipudi [a,b,*], E. Epler [b], C.A. Volkert [b]

[a] School of Minerals, Metallurgical and Materials Engineering, Indian Institute of Technology Bhubaneswar, Arugul, Jatni, Khurda - 752050, Odisha, India
[b] Institut für Materialphysik, Georg-August-Universität Göttingen, Friedrich-Hund-Platz 1, 37077 Göttingen, Germany

ARTICLE INFO

Article history:
Received 8 June 2017
Received in revised form 9 November 2017
Accepted 11 November 2017
Available online 23 November 2017

Keywords:
Nanoporous metals
Multiaxial loading
Yield criterion
Plastic Poisson ratio
Nanotomography

ABSTRACT

We investigate the multiaxial behavior of nanoporous gold (np-Au) using finite element simulations on tomographic reconstructions, and its inferences of the hardness-to-yield strength ratio from nanoindentation and microcompression experiments on np-Au. Plane stress and axisymmetric loading simulations were carried out on real np-Au structures and simulated spinodal structures. The predicted initial yield response of spinodal and np-Au is nearly identical, while disagreeing with the Deshpande-Fleck foam yield criterion. A qualitative comparison of np-Au simulations with Deshpande-Fleck criterion suggests a plastic Poisson ratio of 0.23, corresponding to a hardness-to-yield stress ratio of 2.7 which is in remarkable agreement with experiments.

Nanoporous gold (np-Au) is a new class of cellular material with relative density in the range of 0.25 to 0.5, which places np-Au between low density engineering foams and dense solids. Uniaxial behavior of nanoporous foams has been extensively studied in the recent years, and is found to be in contrast with the macroporous foams. Macroscopic elastic modulus and flow stress of np-Au from nanoindentation and microcompression tests were found to depend on the ligament length scale [1–5], leading to modified size-dependent Gibson and Ashby scaling laws [2,6–8]. Additionally, some experimental and computational studies have suggested a change in the relative density scaling of the elastoplastic properties [9–13] or inclusion of the network topology into scaling relations [14,15]. However, so far there have been no direct multiaxial yielding studies either in experiments or through simulations. While investigating the Poisson effects under uniaxial compression tests on mm-sized samples, Lührs et al. [16] have applied digital image correlation (DIC) and to separate out the effect of barreling they assumed that np-Au obeys Deshpande-Fleck (DF) isotropic foam yield criterion [17]. Perturbed/randomized gyroidal structures, which are sometimes taken as approximations to np-Au, have been shown to depart from the DF yield criterion [18]. Thus, the validity of DF yield criterion to np-Au remains to be verified, which forms one of the goals of this paper.

Another notable difference with the very low density macroporous foams is the ability of np-Au to develop plastic constraints under the indenter. It is understood that cell walls of a low density macroporous foam develop localized plastic hinges near cell wall junctions, and plastically collapse under compression resulting in near-zero plastic Poisson ratio (ν_p). Consequently, the foam below the indenter is under uniaxial compression (except near the indenter edges), and hence, is unable to develop significant plastic constraints [19–21]. This results in the compressive yield strength (σ_Y) being roughly equal to the indentation hardness (H) [20,21]. In contrast, in situ indentation of np-Au in transmission electron microscope showed extended deformation region under the indenter [22]. Hence, a non-zero ν_p may be expected for np-Au under compression, which leads to $H/\sigma_Y > 1$ [23]. In fact, Jin et al. [24] have compared microindentation hardness with compressive yield strength of mm-sized samples and found that $H/\sigma_Y = 3$. This corresponds to incompressible plasticity ($\nu_p = 0.5$), although their measurements yielded $\nu_p = 0.08$ from specimen dimensional changes. In contrast, Volkert et al. [3] reported $\nu_p \approx 0.2$ also from the dimensional changes of a np-Au micropillar in microcompression tests. Recently, Lühr et al. [16] have also used DIC on mm-scale samples under compression and report values between ≈ 0.07 to 0.25 for ligament diameters of 50 to 180 nm and over a range of strains. This would correspond to a H/σ_Y ratio roughly in the range of 1.7–2.8 [23].

A clear convincing relationship between σ_Y and H can be obtained if these are measured from the same sample along with ν_p. Only one such consistent work [24] can be found so far, which however finds an inconsistency between ν_p and H/σ_Y. Interestingly, on mm-scale np-Au, but under tension, Briot and Balk [25] reported that $\nu_p \approx 0.22$ using DIC, and employed $H = 2.65\sigma_Y$ to convert nanoindentation hardness [7] which they found to be in good agreement with tensile yield strength.

* Corresponding author.
E-mail addresses: kodanda@iitbbs.ac.in (K.R. Mangipudi), volkert@ump.gwdg.de (C.A. Volkert).

https://doi.org/10.1016/j.scriptamat.2017.11.033
1359-6462/

However, the tensile ν_p may not necessarily be equal to compressive ν_p to which H/σ_Y is correlated. For example, molecular dynamics (MD) simulations on spinodal structures have predicted a strain-dependent ν_p that can be as high as 0.6 in tension while becoming near-zero under compression [26]. A ductile and very low density foam with near-zero ν_p will have a relatively larger ν_p in tension, since the plastic hinges near the cell wall junctions reorient the cell walls towards the loading axis similar to a pin-jointed structure. Moreover, it is unclear if the ν_p measured in mm-scale samples with multiple np-Au grains and low network connectivity at the grain boundaries is also the ν_p of individual grains where nanoindentation is performed. Measuring ν_p from deformed geometries of micropillars involves difficulties arising from buckling or barreling [3].

In this paper, we also aim to gain more insight into the hardness-to-yield stress ratio of np-Au (i) from nanoindentation and micropillar compression tests on the same sample, and (ii) from ν_p by comparing the multiaxial behavior from finite element (FE) simulations with the DF criterion [17]. If the multiaxial yield response of np-Au obeys DF criterion, this can indirectly estimate ν_p with better accuracy. FE simulations are conducted on reconstructed np-Au from the same sample using focused ion beam (FIB) nanotomography [14,15,27], and also on spinodal structures [14] to obtain the multiaxial yield response, and compare it with the DF yield criterion [17].

Np-Au is produced by the dealloying method outlined in [28]. The average relative density of the sample from densitometry measurements is 0.31 ± 0.005. The np-Au samples produced are free of large voids and cracks. Berkovich nanoindentation and micropillar compression tests are conducted using a MTS 200 Nanoindentor. Berkovich indentation has been performed at a constant indentation strain rate (1%/s) with a superimposed oscillatory signal (45 Hz, 2 nm). Elastic modulus and hardness are calculated using the continuous stiffness method. Microcompression tests are performed using a flat punch indentor on pillars of 10 μm in height and 5 μm in diameter fabricated by FIB. The loading rate is 100 μN/s, and the total applied macroscopic strain is about 20%. The measured force-displacement response is converted to nominal stress-nominal strain curves assuming homogeneous deformation of the pillars.

Fig. 1 shows the elastic modulus and hardness measured from nanoindentation. The rate of decrease in both elastic modulus and hardness beyond an indentation depth of 500 nm is rather small. We report the elastic modulus and hardness values corresponding to an indentation depth of 700 nm. Beyond an indentation depth of 700 nm, the change in modulus or hardness is only a few percent whereas more pronounced sink-in and circumferential cracks tend to form. The average values of the elastic modulus and hardness from 50 or more indents are 1.8 ± 0.1 GPa and 63 ± 4 MPa, respectively. The nominal stress-stain response from micropillar compression tests is shown in Fig. 1(c). The elastic modulus is taken from the initial segment of the unloading curve, and the yield stress is taken as the 0.2% off-set stress given by the average slope of the loading segment as shown in the figure. The unloading modulus is 1.2 ± 0.2 GPa which is lower than the modulus from nanoindentation. The off-set yield stress is 23 ± 1 MPa, which differs from the indentation hardness by a factor of 2.7 to 2.8.

For FE simulations, the three-dimensional structure of $(1250\ \text{nm})^3$, shown in the inset of Fig. 2, is obtained using FIB nanotomography described in [27]. We repeat these simulations also on spinodal structures generated through a phase-field model [14], which are morphologically similar but differ in topology [14]. The relative density of both the structures is ~0.3.

FE simulations were performed using ABAQUS [29] and CalculiX [30]. For both reconstructed and spinodal structures, the ligament material is assumed to be elastically and plastically isotropic, a perfectly plastic material and obeys J_2-flow theory. For simplicity, we neglect the crystallographic nature of plastic yielding in the ligaments. We also assume that the flow stress of the solid is independent of the local diameter of the ligaments. We take 79 GPa for the elastic modulus, and 0.42 for the Poisson ratio, which are literature values for isotropic bulk gold. We use 750 MPa for the flow stress of the ligament material. These assumptions are reasonable since we limit our focus only up to macroscopic early yielding of np-Au and due to the fact that the orientation of ligaments results in isotropic mechanical response independent of the shared crystallographic orientation [12,28,31]. The gold volume is meshed using quadratic tetrahedral elements. Within the statistical scatter expected for random cellular materials, the uniaxial elastoplastic response of the structure in the inset of Fig. 2 is found to be free from sample size effects from stress-free lateral boundaries [32].

Uniaxial tensile simulations are performed by prescribing normal displacements together with roller boundary conditions on one set of opposite faces. The macroscopic stress components on the sample are obtained by dividing the sum of the appropriate nodal reaction force components on each boundary by the corresponding boundary area (area of solid and pores). The uniaxial elastic moduli, E, along the three directions have been found to be 1.86 GPa, 1.88 GPa, and 1.68 GPa, displaying slight anisotropy of 0.9 along the Z-direction which is the slicing direction during nanotomography. It is known that the nanotomography method produced an artifact of slight structural anisotropy of 0.9 along the slicing direction due to relatively large slice thickness [27], which explains the slight Z-anisotropy in E since the modulus varies roughly linearly for small structural anisotropies [32,33]. The same is also suggested by the evolution of stress components (Fig. 2) during hydrostatic loading by equal straining along the three coordinate directions. Hence, it may be reasonable to

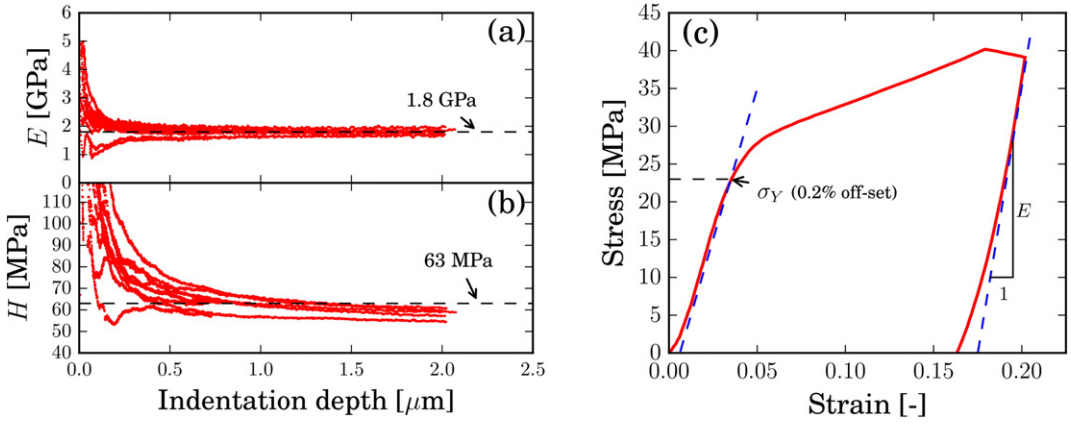

Fig. 1. (a) and (b) Variation in the elastic modulus E and hardness H with indentation depth during nanoindentation. The mean values of the modulus and hardness at an indentation depth of 700 nm are also indicated. (c) Nominal stress-nominal strain curve from microcompression test. The elastic modulus is taken from the slope of the unloading segment, while the yield stress is taken as the 0.2% off-set stress obtained using average slope of the initial loading segment.